Chapter 11
Transport of Reactive Contaminants

The previous chapter focused on the physical mechanisms (advection, diffusion, and dispersion) and the physical characteristics of the subsurface (heterogeneity) that control the dynamics of contaminant transport from the land surface to the water table. In addition, contaminants are subject to a range of chemical interactions with other (dissolved) chemical species present in the subsurface, colloids, and the porous matrix itself. The previous sections of this book dealt with such reactions, including sorption (by various types of bonding), decay, degradation, complexation, precipitation, dissolution, and volatilization as well as interactions (and transport) with migrating colloids. These reactions thus influence—and are influenced by—advective, diffusive, and dispersive transport mechanisms. To include the effects of these reactions in quantifying the dynamics of contaminant transport, additional terms can be included in the transport equations surveyed in Chap. 10. In most cases, the resulting transport equations contain relatively simple terms that account for chemical species loss from or entry to the aqueous solution.

It should be emphasized that, to date, the ability to quantify the complex chemical reaction phenomena that occur in the subsurface and also integrate the variability in flow behavior caused by natural heterogeneity and fluctuating boundary (land surface) conditions remains very limited. As a consequence, developing and improving the predictive capabilities of models are the areas of active research.

11.1 Contaminant Sorption

Sorption of contaminants can be included in the advection–dispersion equation by introducing a retardation factor:

$$\frac{\partial}{\partial t}\left(c + \frac{\rho_b S}{\theta}\right) = \frac{\partial}{\partial x}(vc) + \frac{\partial}{\partial x}\left[D_h \frac{\partial}{\partial x}\right], \tag{11.1}$$

B. Berkowitz et al., *Contaminant Geochemistry*,
DOI: 10.1007/978-3-642-54777-5_11, © Springer-Verlag Berlin Heidelberg 2014

where ρ_b denotes bulk mass density of the porous medium and S is the adsorbed phase concentration. The sorbed phase S subsequently is quantified in terms of an isotherm, as discussed in Chap. 5. Usually, the simple linear Freundlich isotherm is assumed to be valid, so that $S = K_d c$, where K_d is the distribution coefficient (or sorption coefficient). More complicated adsorption–desorption terms can be incorporated, for example, for the case of different forward and reverse sorption rates. Then, Eq. (11.1) can be written in terms of a retardation coefficient, R, in the form

$$R\frac{\partial c}{\partial t} = -\frac{\partial}{\partial x}(vc) + \frac{\partial}{\partial x}\left[D_h \frac{\partial}{\partial x}\right], \tag{11.2}$$

where

$$R \equiv 1 + \frac{\rho_b K_d}{\theta}. \tag{11.3}$$

Thus, the travel time for an adsorbed chemical, t_a, can be related to the travel time for a mobile, conservative (nonsorbing) chemical, t_a, by

$$t_a = (1 + \rho_b K_d/\theta)t_m \equiv Rt_m. \tag{11.4}$$

Equation (11.4) also can be written as $v_a = vR$, where v_a denotes the average velocity of a sorbing contaminant. Thus, the concentration profile of a sorbing contaminant is retarded, relative to a nonsorbing contaminant, as shown schematically in Fig. 10.1c.

Sorption can be included in the more general CTRW transport equation discussed in Sect. 10.3. Margolin et al. (2003) show the relation between macroscopic transport behaviors of passive and sorbing (reactive) tracers in heterogeneous media. In the framework of CTRW, they formulate the sorption process using a "sticking" rate and a "sticking" time distribution and derive a relation between the distributions of the sorbing and nonsorbing tracer in terms of these quantities. Alternatively, sorption can be included directly in the definition of the transition time distribution, ψ(s, t). This approach is valid when chemical sorption acts only as a relatively gentle "modifying" mechanism on the overall transport, in which the long-time tail in a breakthrough curve is further delayed. In other physical situations, however, transport may be governed by two highly distinct rate spectra for transport, such as reactive tracers undergoing (slow) sorption (adsorption–desorption) during migration in a heterogeneous advective flow field (e.g., Starr et al. 1985). Berkowitz et al. (2008) show that this "two-scale" behavior can be quantified by appropriate modification of the governing transport equation.

Regardless of the transport equation considered, the major effect of sorption on contaminant breakthrough curves is to delay the entire curve on the time axis, relative to a passive (nonsorbing) contaminant (Rubin et al. 2012). Because of the longer residence time in the porous medium, advective–diffusive–dispersive interactions also are affected, so that longer (non-Fickian) tailing in the breakthrough curves is often observed.

11.2 Colloids and Sorption on Colloids

In previous chapters, we discussed the role of colloids and colloid-like materials, as both carriers of adsorbed chemicals and contaminants in their own right. It is well recognized that contaminants farther can interact with and adsorb onto migrating colloids, and thus advance much farther or deeper into the subsurface than would be expected if the role of colloids were ignored (e.g., Saiers and Hornberger 1996). For example, an organic colloid particle can act as a sorbent for a neutral organic molecule, thus facilitating advective transport of the neutral molecule.

In this situation, transport equations similar to those discussed previously can be applied. For example, by assuming sorption to be essentially instantaneous, the advective–dispersion equation with a reaction term (Saiers and Hornberger 1996) can be considered. Alternatively, CTRW transport equations with a single ψ(s, t) can be applied or two different time spectra (for the dispersive transport and for the distribution of transfer times between mobile and immobile—diffusion, sorption—states can be treated; Berkowitz et al. 2008; Bijeljic et al. 2011).

The transport of colloids in porous media is usually considered to be controlled by four mechanisms: advection, dispersion, straining, and physicochemical particle–surface interactions (McDowell-Boyer et al. 1986; Ryan and Elimelech 1996); see also Sect. 5.7.3. *Straining* refers to the permanent physical trapping of colloids in narrow pore throats and is a key mechanism, particularly in porous media with grain diameters smaller than 20–50 times the colloid diameter (McDowell-Boyer et al. 1986). Physicochemical interactions with the porous medium occur when colloids approach grain surfaces due to pore-scale diffusion, sedimentation, or inertial forces. These interactions lead to permanent or temporary attachment to the porous medium solid phase and are controlled by electrostatic forces (including London–van der Waals forces). Such electrostatic forces are explained in terms of electric double-layer theory (Israelachvili 1991). Particles deposit in the secondary energy minimum of the electric double layer at the grain surface. Moreover, deeper secondary minima closer to the solid surfaces occur at higher ionic strength (Redman et al. 2004). Thus, changes in solution chemistry promote colloid mobilization (deposition) by altering the double-layer potential energy.

The transport behavior of colloids commonly is modeled by colloid filtration theory (CFT) (Yao et al. 1971), which is based on extension of the common advection–dispersion equation. The one-dimensional advection–dispersion–filtration equation is written

$$\frac{\partial c}{\partial t} = -v\frac{\partial c}{\partial x} + \frac{\partial}{\partial x}\left[D_h \frac{\partial c}{\partial x}\right] - \lambda v c \tag{11.5}$$

where λ is known as the filtration coefficient, which is assumed to be constant in time and space. The CFT allows determination of λ from the physical properties of the colloid and the porous medium:

$$\lambda = \frac{3}{2}(1-n)\frac{L}{d_c}\alpha_c\eta, \tag{11.6}$$

where n is the porosity, L is the length of the porous medium column, d_c is the median grain size diameter (Rajagopalan and Tien 1976), α_c is the collision efficiency (an empirical, fitting constant), and η is the collector efficiency (estimated by various means, as discussed by Logan et al. (1995) and Tufenkji and Elimelech 2004. The CFT assumes homogeneity of particles and the porous matrix and leads to an expected fast exponential concentration decay along the colloid travel path. The CFT can be modified to account for the occurrence of nonideal behavior, for example, by combining Eq. (11.5) with a model for a first-order, rate-limited adsorption–desorption process (Eq. 11.1) (Toride et al. 1995).

A major problem with these approaches, however, lies in the complexity and nonuniqueness involved with identification of parameterizations for processes of particle straining, deposition, and detachment. An alternative to CFT-based theories is given by Amitay-Rosen et al. (2005), who suggest a simple phenomenological model of particle deposition and porosity reduction that avoids these difficulties.

As noted by Cortis et al. (2006), CFT and modifications of standard filtration models invariably predict an exponential decay of the colloid concentration with distance. However, similar to the discussion of non-Fickian transport in Sect. 10.3, power-law tails in breakthrough curves are observed frequently in experiments (e.g., in the context of bacterial "biocolloids," see Albinger et al. 1994; Martin et al. 1996; Camesano and Logan 1998; Baygents et al. 1998; Bolster et al. 1998; Redman et al. 2001). Cortis et al. (2006) propose a generalized model based on CTRW theory that captures these power-law tails, together with the full evolution of breakthrough curves. The CTRW filtration model is found to be controlled by three parameters, which are related to the overall breakthrough retardation (R), the slope of the power-law tail (β), and the transition to a decay slower than t^{-1}.

11.3 Dissolving and Precipitating Contaminants

Dissolution and precipitation can occur as contaminants travel from the land surface to groundwater aquifers. These processes can affect water chemistry, and they can significantly modify the physical and chemical properties of porous media (Lasaga 1984; Palmer 1996; Dijk and Berkowitz 1998, 2000; Darmody et al. 2000). Under some conditions, large quantities of mass can be transferred between the liquid and solid mineral phases.

A number of experimental and theoretical studies analyzed the influence of dissolution processes on the physical and chemical properties of soluble porous matrices (Fogler and Rege 1986; Daccord and Lenormand 1987; Hoefner and Fogler 1988; Daccord 1987; Daccord et al. 1993). Similarly, several theoretical

studies provided some understanding of the evolution of hydraulic conductivity caused by precipitation processes (Novak and Lake 1989; Novak 1993; Bolton et al. 1996, 1997, Dijk and Berkowitz 1998).

Loss or gain of dissolved chemical species from soil water by precipitation or dissolution, respectively, usually is accounted for by adding a simple sink-source term in the advection–dispersion equation:

$$\frac{\partial}{\partial t}(\theta c) = -\frac{\partial}{\partial x}(v\theta c) + \frac{\partial}{\partial x}\left[D_h\theta\frac{\partial c}{\partial x}\right] - \sum_{i=1}^{n} Q_i, \tag{11.7}$$

where Q_i denotes sink (or source) terms that account for, for example, contaminant degradation, plant uptake, volatilization, or precipitation (dissolution). Alternatively, focusing on precipitation–dissolution at the pore scale, the hydrodynamic dispersion coefficient D_h can be replaced by the coefficient of molecular diffusion, so that Eq. (11.7) can be applied as an advection–diffusion equation.

Dissolution is a relatively simple mechanism, and so application of an advection–diffusion equation modified by a source term, or a similarly modified non-Fickian (CTRW) transport equation (Hornung et al. 2005), can effectively capture chemical transport patterns. On the other hand, the interplay between the chemical and physical aspects of mineral precipitation is more complex. In some instances, during infilling of fissures and pore spaces by mineral precipitation, porosity is reduced uniformly; in other cases, pockets of high porosity or unfilled fissures may remain. In addition to the chemical kinetics of precipitation, the flow dynamics and transport also are important factors in determining the resulting patterns of porosity and mineral deposition (Dijk and Berkowitz 1998). Note also that modeling approaches similar to those for treating precipitating contaminants can be employed to account for degradation and volatilization of contaminants in water.

For a given mineral to precipitate, a solution must be oversaturated with respect to the mineral being deposited (i.e., the ion product must exceed the solubility product), and the precipitation process must be kinetically favorable. The most "conventional" model for describing the deposition of minerals within rock formations maintains that supersaturated fluids pass through a porous or fractured rock, precipitating minerals along the way. However, recent experimental studies demonstrate that a number of difficulties are inherent in such a simplified picture of mineralization. Lee and Morse (1999) and Hilgers and Urai (2002) found that when supersaturated fluids flowed through artificial fractures, most of the mineral deposition occurred within several centimeters of the inlet.

Fluids become supersaturated, and thus, mineral deposition occurs, by three main mechanisms: (1) changes in fluid pressures and temperatures during flow through the porous medium, (2) dissolution of a particular mineral in the matrix that results in the fluid being supersaturated with respect to another mineral (e.g., dissolution of calcite and precipitation of gypsum; Singurindy and Berkowitz 2003), and (3) mixing-induced supersaturation. This third mechanism occurs when two initially saturated or undersaturated fluids of different chemical compositions

or temperatures are mixed, resulting in a new solution that is oversaturated. While widely discussed in the geochemical literature, only limited reference to mixing-induced precipitation has been made in hydrological studies.

In addition to considering the mode by which supersaturation is reached, the physical changes in the rock resulting from precipitation also crucially affect the dynamics of precipitation. Porosity can be reduced by crystal growth, and this can have an effect on additional physical parameters in the porous matrix, such as the specific surface area. Both porosity and specific surface area are important parameters in subsurface systems, as they determine to a large extent both the permeability of the rock and the chemical kinetics of mineral precipitation. Therefore, both porosity and specific surface area must be incorporated into mass conservation and transport equations. Changes in porosity can be related to the volumetric changes in the amount of mineral precipitated in a relatively straightforward manner, but changes in specific surface area are more difficult to quantify.

One approach to quantitatively relate changes in porosity to changes in specific surface area is to assume that the porous medium is composed of spherical grains. The resulting specific surface area per unit volume of rock $\bar{s}$, is related to the porosity, ϕ, by the relationship (Lichtner 1988)

$$\bar{s} = \bar{s}_{\mathrm{o}} \left(\frac{1-\phi}{1-\phi_{\mathrm{o}}} \right)^{2/3}, \tag{11.8}$$

where $\bar{s}_{\mathrm{o}}$ is the specific surface area of the rock at a porosity of ϕ_{o}. Alternatively, if it is assumed that the pores can be approximated by spheres, the specific surface area can be expressed by Kieffer et al. (1999)

$$\bar{s} = \bar{s}_{\mathrm{o}} \left(\frac{\phi}{\phi_{\mathrm{o}}} \right)^{2/3}. \tag{11.9}$$

Therefore, in the first model, the specific surface area increases with decreasing porosity, while in the second, the opposite relationship is specified. While some attempts have been made to experimentally verify these models in individual rock types (Kieffer et al. 1999; Jové Colon et al. 2004), the data concerning a wide range of rocks and precipitation–dissolution reactions remain limited.

Emmanuel and Berkowitz (2005) examined the dynamics and patterns of changing porosity during mixing-induced precipitation, using a two-dimensional numerical model that simulates mixing-induced precipitation in both homogeneous and heterogeneous porous media. The role of specific surface area also was explored. The precipitation of a and b in equimolar amounts to form a solid ab was considered, a scenario that ensures that $R_a = R_b$. The sink term can then be assumed to have the generic form often valid for near-equilibrium conditions (Morse and Arvidson 2002):

$$R = -\bar{s}K_r\left(\frac{C_a C_b}{K_{sp}} - 1\right)^n, \tag{11.10}$$

where K_r is a kinetic rate coefficient, K_{sp} is the solubility product of the solid ab, and n is an empirical reaction order. The rate of change of porosity can be derived from the sink term by dimensional analysis. As R is defined as the number of moles precipitated per unit time per unit volume of fluid, multiplying by both porosity and molar volume (M_v) yields the volumetric rate of change of precipitated material per unit volume of bulk matrix:

$$\frac{\partial \phi}{\partial t} = \phi M_v R. \tag{11.11}$$

Equation (11.10) is valid for near-equilibrium systems, so that it can be applied to mass-transfer-limited processes, that is, systems in which the large-scale rate of change of porosity is limited by the solute flux rather than the reaction kinetics.

Application of this model showed that the complete reduction in porosity near the inlet does not lead to clogging of a system: nonsupersaturated fluids are able to flow around closed regions and into more permeable areas where mixing and subsequent deposition can occur. Thus, mixing-induced precipitation is expected to reduce porosity in concentrated regions rather than lead to evenly precipitated material throughout the porous domain.

11.4 Transport of Immiscible Liquids

Petroleum products, synthetic organic solvents, and other toxic organic compounds dissolved in organic solvents, generally referred to as nonaqueous phase liquids (NAPLs), are a key class of contaminants in the subsurface. These compounds are generally insoluble or only slightly soluble in water. As a consequence, NAPLs remain as distinct liquid phases as they are transported downward from land surface to the water table; this migration is governed mostly by the density and viscosity of the NAPL. Specific contaminants often are classified as dense NAPLs (DNAPLs), such as trichloroethylene and carbon tetrachloride, or as light NAPLs (LNAPLs), such as oil and gasoline, according to their density relative to water. DNAPLs sink through the water table region, downward through the fully saturated zone, while LNAPLs remain in the capillary fringe, "floating" on the surface of the free water. A schematic illustration of LNAPL and DNAPL transport from land surface is shown in Fig. 11.1.

Figure 11.1 provides only a coarse-level picture of NAPL migration. Depending on the viscosity and density ratios, between the NAPL and the resident water, as well as the properties (physical and chemical) of the porous medium, a variety of (unstable) fingering and (stable) fronts can develop with depth. More specifically, the degree of fingering in the displacement and the actual rate of downward (and

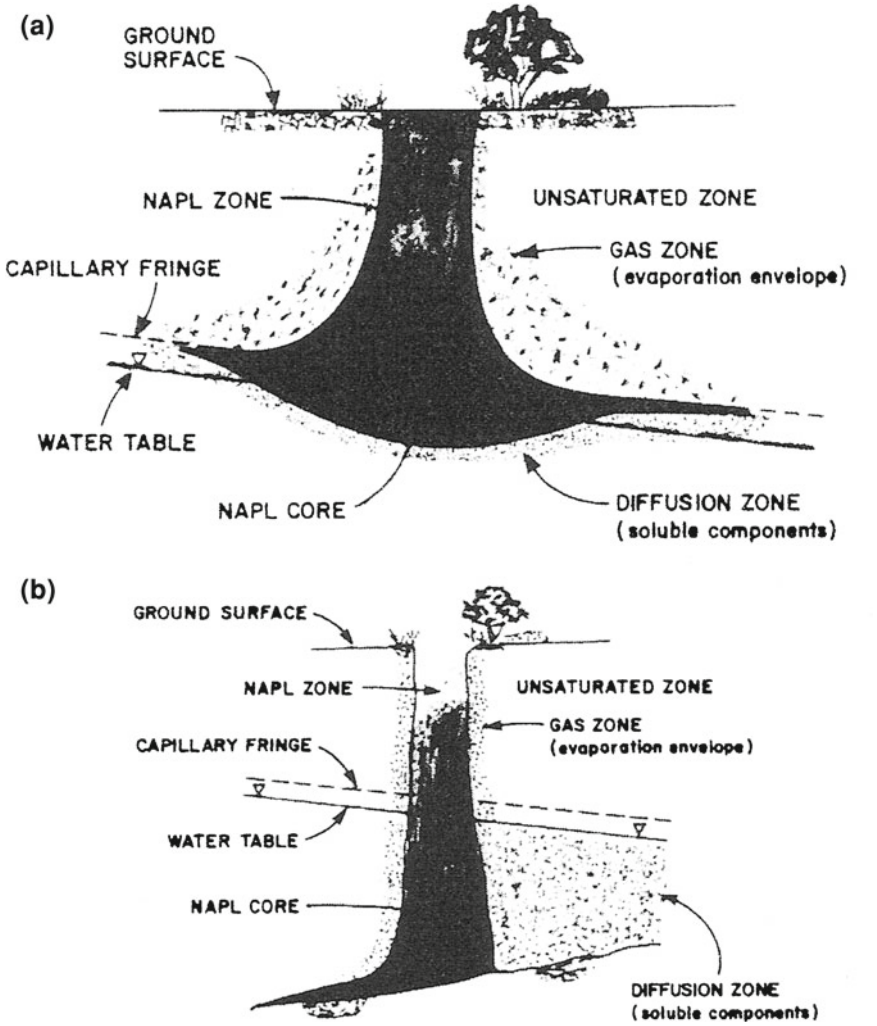

Fig. 11.1 Schematic representation of NAPL movement from land surface to the water table region. **a** LNAPL movement and **b** DNAPL movement (Abriola and Pinder 1985). Reproduced by permission of American Geophysical Union. Abriola and Pinder (1985), Copyright 1985, American Geophysical Union

lateral) migration are governed by (1) the properties (e.g., surface wetting) of the NAPL itself, (2) the NAPL density and viscosity relative to the resident pore water, (3) the actual moisture content, (4) the properties (physical, such as pore size, and chemical, such as wettability) of the porous matrix, and (5) the inlet/infiltration condition and NAPL volume (Schwille 1988). Volatilization of components in the NAPL also affects the rate and pattern of migration, as properties of surface wetting, density, and viscosity change over time. Figures 11.2 and 11.3 show migration

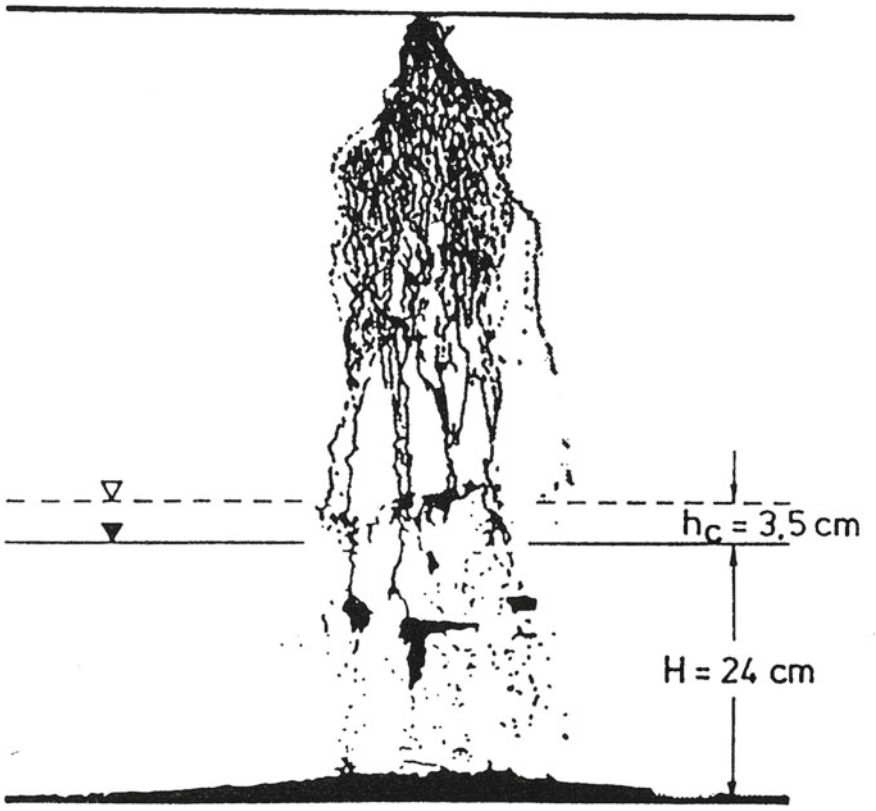

Fig. 11.2 Infiltration pattern of a DNAPL in an heterogeneous domain, through the partially saturated, capillary fringe, and saturated zones; h_c and H represent the heights of the capillary fringe and the saturated zone, respectively (Schwille 1988)

patterns from two experiments, in heterogeneous and homogeneous domains. The different fingering patterns are clearly observed.

In partially saturated media, the moisture content affects NAPL migration significantly. Abriola and Pinder (1985) suggested that the flux of a phase p (NAPL, water, or air), J_p, can be written as

$$J_p = -k_p K_{\mathrm{sp}}^h \left[\frac{\mathrm{d}h_p}{\mathrm{d}x} + \frac{\rho_p}{p^*} \right], \tag{11.12}$$

where k_p is the relative permeability of phase p in the porous matrix, K_{sp}^h is the saturated hydraulic conductivity for phase p in the matrix, h_p is the pressure head of phase p, ρ_p is the density of the phase p, and p^* is a scaled reference phase density. Clearly, the actual pressure head in each phase depends on the fluid configuration within the pores. Flux equations for each of the three phases can be

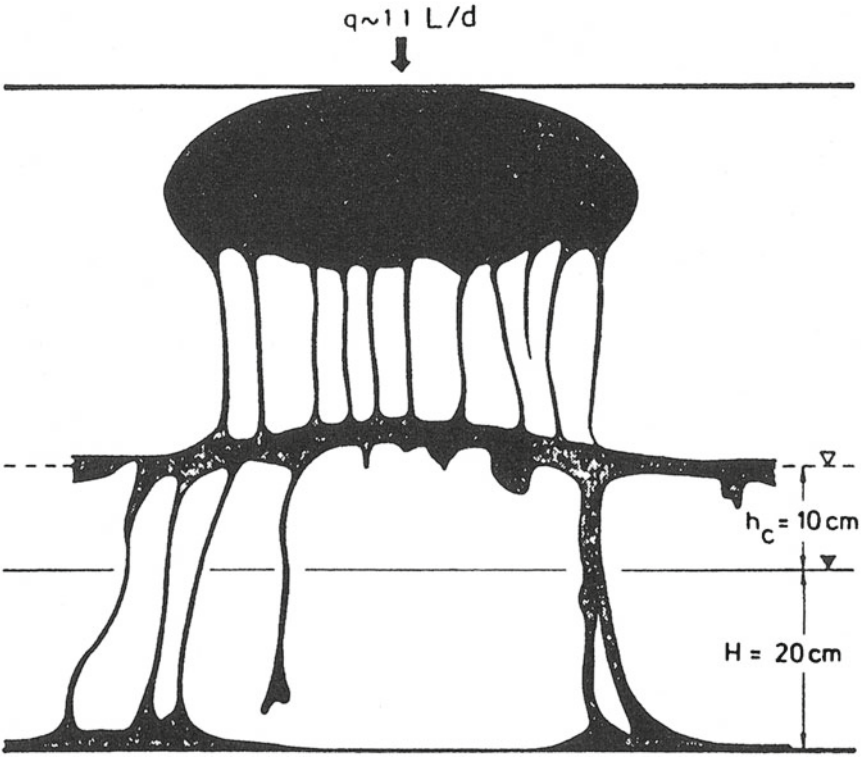

Fig. 11.3 Infiltration pattern of a DNAPL in an homogeneous domain, through the partially saturated, capillary fringe, and saturated zones; h_c and H represent the heights of the capillary fringe and the saturated zone, respectively (Schwille 1988)

combined with mass conservation equations to derive governing transport equations.

The relative permeability is difficult to quantify. It usually is estimated on the basis of laboratory experiments, as a function of relative saturation. In three-phase NAPL–water–air systems, each relative permeability is dependent on the relative saturation of each of the phases. Modeling based on empirical considerations can be employed. For example, Blunt (2000) discusses a model to estimate three-phase relative permeability, based on saturation-weighted interpolation of two-phase relative permeabilities. The model accounts for the trapping of the NAPL and air (gas) phases and predicts three-phase relative permeabilities for different porous medium and NAPL properties. However, experimental determination of two- and three-phase relative permeabilities is a particularly complex issue that remains a subject of basic research.

Another aspect of NAPL migration in the subsurface environment, different from movement of dissolved contaminants, is that, as it advances downward through the partially saturated zone, a fraction of the NAPL phase remains trapped

in some pores, as a coating on pore walls and as microdroplets trapped within pore spaces by interfacial surface tension. This NAPL fraction is referred to as the *residual saturation.* The presence of this fraction may contribute volatilized phases and dissolved components during subsequent water infiltration and redistribution. In addition, if the residual fraction is hydrophobic, its presence further affects subsequent water and contaminant movement. The flow and distribution of the liquid phases are controlled by the movements of the interfaces between the nonwetting and wetting phases that result from changes in pressure and saturation (Blunt and Scher 1995; Reeves and Celia 1996; Cheng et al. 2004).

Quantification of NAPL transport usually is considered by using advection–dispersion equations for each of the water and NAPL phases and defining relative permeabilities (as noted previously). Alternatively, if the emphasis is on contamination of water from a dissolving NAPL source (e.g., from residual NAPL in the vadose zone or NAPL pools and localized leaks), then transport equations containing a simple source term, such as Eq. (11.7), can be considered.

The previously mentioned approaches are useful when quantification at the average ("effective") continuum ("macroscale") level is appropriate. However, pore-scale network models are more appropriately used to examine fluid distribution within pores and clusters of pores (recall Sect. 9.1). NAPL migration through the vadose zone undergoes significant fingering (unstable infiltration), and because it is a nonwetting liquid relative to the solid phase (and immiscible in water), NAPL displacement of water is in effect a drainage process, as discussed in Sect. 9.1. Pore-scale information such as NAPL geometry or interfacial configuration (or the interfacial area between the nonwetting and wetting liquids) is important (Miller et al. 1990; Powers et al. 1992; Cheng et al. 2004; Ovdat and Berkowitz 2006). Knowledge of this interfacial area is particularly useful for quantifying processes such as contaminant adsorption, dissolution, volatilization, and enhanced oil recovery (Reeves and Celia 1996; Saripalli et al. 1997; Johns and Gladden 1999; Schaefer et al. 2000; Jain et al. 2003). NAPL migration at the pore scale is illustrated in Fig. 11.4.

At the pore level, fluids are conveniently characterized by three main parameters. The viscosity ratio is given by $M = \mu_d/\mu_r$, where μ_d and μ_r are the viscosities of the displacing and resident fluids, respectively, while the capillary number is defined as $\mathrm{Ca} = \mathrm{q}\mu_d/\gamma$, where q is the specific discharge of the displacing fluid and γ is the interfacial tension. The bond number, $\mathrm{Bo} = gr^2\Delta\rho/\gamma$, where g is the gravitational acceleration, r is the characteristic pore radius, and $\Delta\rho$ is the fluid density difference, is then introduced to account for buoyancy-gravity forces. The usual convention is that $\mathrm{Bo} > 0$ (dense fluid displaced by light fluid) stabilizes the interface, whereas $\mathrm{Bo} < 0$ (light fluid displaced by dense fluid) destabilizes it.

Lenormand et al. (1988) pioneered experiments on immiscible displacements in two-dimensional, artificial porous media, using horizontal models with negligible inertial and gravity forces and developed a numerical model to describe fluid displacement in such porous media, accounting for capillary and viscous forces. Comparison between the experiments and numerical simulations led Lenormand

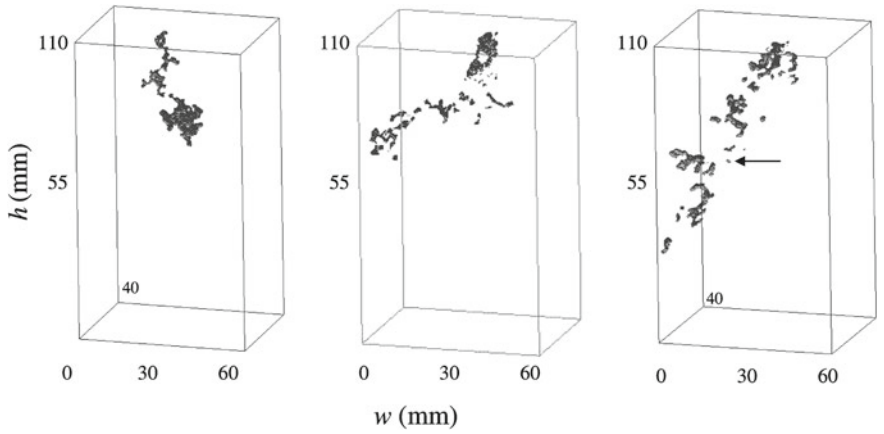

Fig. 11.4 Pore-scale, three-dimensional images of nonwetting fluid invading a wetting fluid, under different conditions of capillary and buoyancy-driven forces and for a similar injected volume. The invasion behavior is characterized by a wide range of displacement patterns and fragmented clusters, one of which is indicated by an *arrow*. (Ovdat and Berkowitz 2006) Reproduced by permission of American Geophysical Union. Ovdat H, Berkowitz B (2006)

et al. (1988) to define a Ca-*M* phase diagram that specifies regions in which stable and unstable displacements occur. At high *M* and low Ca, capillary-driven fingering occurs, whereas at low *M* and high Ca, viscous fingering dominates. Ewing and Berkowitz (1998) extended this phase diagram to three dimensions to account for buoyancy-gravity forces.

We note also that invasion percolation (IP) models (Wilkinson and Willemsen 1983; Furuberg et al. 1988) have been used extensively to simulate the slow displacement of a wetting fluid by a nonwetting fluid in porous media, when capillary forces dominate over viscous forces. In such models, the fluid–fluid displacement process is represented by a cluster growth process on a lattice that at breakthrough generates a self-similar fractal. The IP algorithm generates structures that quantitative analysis reveals to be similar to patterns formed during fluid–fluid displacement processes. While the IP model originally was developed for neutrally buoyant systems, accounting for capillary forces, it has since been modified to include the effects of buoyancy on the drainage process (Wilkinson 1984, 1986). Lenormand and Zarcone (1985) measured directly the structure of injected clusters in transparent resin used as porous media.

Finally, it should be noted that NAPL infiltration is accompanied by dissolution of some components into the aqueous phase, volatilization of other components into the air phase of the partially saturated zone, and possibly organic complexation with resident soil (Jury and Fluhler 1992). Mass flux of volatilized phases in the near surface can be included in transport equations, as discussed in Sect.11.3.

11.5 Transport of Contaminants by Runoff

11.5.1 Overland Runoff

The fraction of rainfall or irrigation water that flows over a land surface from higher to lower elevations, known as *overland runoff,* is an additional pathway for contaminant transport. Runoff occurs when the amount of rain or irrigation water is greater than the soil infiltration capacity. The formation of a crust on the soil surface is a major contributor to runoff formation in arid and semiarid zones, because it decreases the infiltration capacity. The soil crust is a thin layer (0–3 mm) with a high density, fine porosity, and low hydraulic conductivity compared to the underlying soil. This "skin" forms as a result of falling raindrops or sodification of soil clays.

Overland runoff may be expressed as a conservation of mass in a flow domain, where the excess rainfall or irrigation rate, R_e, is equal to the difference between the rainfall and infiltration rates:

$$R_{\mathrm{e}} = \frac{\partial h}{\partial t} + \nabla \cdot q, \tag{11.13}$$

where h is the flow depth and q is the unit discharge. The excess rainfall may be determined directly, while the infiltration rate may be estimated by empirical or physical models. Equation 11.13 is adjusted to consider spatial variability and land hydraulic properties, to reduce errors in estimating runoff infiltration (Wallach et al. 1997; Michaelides and Wilson 2007).

After sediment has been detached by rainfall impact during an erosion event, the majority of it returns to the soil surface after being carried some distance downslope. Through the continuous addition of sediment to the water layer, by impact of raindrops, fine sediment forms a "suspended load" with a settling velocity less than the typical velocity of whirling eddies in flowing water. This velocity is called the *friction velocity* (Rose 1993). The rate of deposition, d_i, defined as the mass of sediment reaching the soil surface per unit area per time (kg/m^2/s), is given by

$$d_i = v_i c_i, \tag{11.14}$$

where c_i is the sediment concentration and v_i is the settling velocity. The rate of rainfall detachment and redetachment is proportional the rainfall rate, raised to some power that has been found empirically to be close to unity (Hairsine and Rose 1991).

When water flows over a contaminated land surface, pollutants released from higher elevations are transported, as dissolved solute or adsorbed on suspended particles, and accumulate at lower elevations. This behavior is reflected in the

spatial variability of contaminant concentration, which affects contaminant redistribution with depth following leaching. If a sorbed contaminant is not of uniform concentration across all soil-size ranges but is higher in the fine sediment fraction, the deposition of this soil fraction controls contaminant redistribution in the subsurface.

The extent of transport of dissolved contaminants in overland runoff is controlled by the topography and morphology of the land (also affected by anthropogenic activity), the depth of chemical incorporation into soil, and the time between rainfall initiation and surface runoff commencement. In addition to these factors, transport of adsorbed contaminants on suspended particles is affected by rainfall intensity, which favors soil erosion.

In general, soluble and nonreactive contaminants are found mainly in dissolved form in runoff water. For example, a large percentage (up to 90 %) of the most soluble herbicides present in the soil layer may be partitioned in overland flowing water. A substantial portion of dissolved nitrogen (8–80 %) and phosphorus (7–30 %) also may be transported in runoff water (Menzel et al. 1978; Hubbard et al. 1982; McDowell et al. 1984). Experiments comparing concentrations of soluble bromide in overland runoff water, as a function of soil type, infiltration rate, and contaminant incorporation depth, under similar "rainfall" conditions, ranged from 0.1 to 14 % (Ahuja 1982; Ahuja and Lehman 1983). Bromide was released to runoff from depths up to 2.0 cm, and concentrations decreased exponentially below the thin crust layer. In treatments where infiltration was impeded due to the presence of a deeper clay layer, the amount of bromide in the runoff water was greater than in treatments with a high infiltration rate. The authors suggested that the mechanism of chemical transfer from below the soil surface to runoff is through a turbulent diffusion process caused by raindrop impact. Based on field experiment results, Walton et al. (2000) stated that the type of soil and its hydraulic and structural properties are the main factors that determine the amount of bromide transported in runoff water. These results are in agreement with Wallach et al. (1997), who quantify overland flow and total runoff volume by considering a spatially variable infiltration rate along the slope. The effect of spatial variability of infiltration on the uncertainty in predicting runoff from sites with distinct topographic characteristics was discussed by Michaelides and Wilson (2007). They found that increasing the range of spatial correlation of infiltration rates leads to increased uncertainty in modeled runoff.

A reactive contaminant may be adsorbed on the soil surface prior to rainfall then, following rainfall that causes erosion, the soil is transported by runoff water in the form of suspended particles redistributed on the land surface. In general, the settling velocity distribution during runoff indicates that the finer particles are resettled initially (Proffitt et al. 1991), although the details of the settling process are affected by different environmental factors, such as soil type and rainfall rate.

11.5.2 Urban Runoff

Urban (municipal) runoff contaminants like surfactants, pesticides, and pharmaceutical products and contaminants associated with highway construction and maintenance are nonpoint sources that contribute significant amounts of pollution to the land surface and thus, indirectly, to the subsurface. Runoff pollution is associated with rainwater or melting snow, which washes impermeable urban surfaces as roads, bridges, parking lots, and rooftops. Suspended solids carried by runoff water represent the major source of urban contamination. For example, Wiesner et al. (1995) estimates that over 40 % of the suspended solids entering Galveston Bay (Texas) are of urban origin. Particle size distributions in runoff, taken under storm and ambient conditions, show that more than 90 % of the particles are between 0.45 and 2 μm. The particulate phase includes 1–10 % organic carbon, with heavy metal functional groups containing detectable levels of Fe, Ba, Cu, Mn, Pb, and Zn. Zinc and barium were distributed bimodally with respect to the size fractions, while lead and iron were associated almost exclusively with the largest size fraction. These results show that suspended particles from runoff include heavy metals. The association of heavy metals with different sizes of suspended particles may affect their spatial distribution on the disposal areas.

A wide range of transport models are available for predicting water contamination and flow under urban runoff. Models based on conventional methods for runoff generation and routing were reviewed critically by Eliott and Trowsdale (2007). These authors suggest that future models on urban runoff should include a broad range of contaminants and improve the representation of contaminant transport.

References

Abriola LM, Pinder GF (1985) A multiphase approach to the modelling of porous media contamination by organic compounds. Water Resour Res 21:11–18

Ahuja LR (1982) Release of soluble chemicals from soil to runoff. Trans Am Soc Agric Eng 25:948–953

Ahuja LR, Lehman OR (1983) The extent and nature of rainfall-soil interaction in the release of soluble chemicals. J Environ Qual 12:34–44

Albinger O, Biesemeyer BK, Arnold RG, Logan BE (1994) Effect of bacterial heterogeneity on adhesion to uniform collectors by monoclonal populations. FEMS Microbiol Lett 124:321–326

Amitay-Rosen T, Cortis A, Berkowitz B (2005) Magnetic resonance imaging and quantitative analysis of particle deposition in porous media. Environ Sci Technol 39:7208–7216

Baygents JC, Glynn JRJ, Albinger O, Biesemeyer BK, Ogden KL, Arnold RG (1998) Variation of surface charge density in monoclonal bacterial populations: implications for transport through porous media. Environ Sci Technol 32:1596–1603

Berkowitz B, Emmanuel S, Scher H (2008) non-Fickian transport and multiple rate mass transfer in porous media. Water Resour Res 44: doi:10.1029/2007WR005906

Bijeljic B, Rubin S, Scher H, Berkowitz B (2011) Non-Fickian transport in porous media with bimodal structural heterogeneity. J Contam Hydrol 120(121):213–221
Blunt MJ (2000) An empirical model for three-phase relative permeability. SPE J 5:435–445
Blunt MJ, Scher H (1995) Pore-level modeling of wetting. Phys Rev E 52:6387–6403
Bolster CH, Hornberger GM, Mills AL, Wilson JL (1998) A method for calculating bacterial deposition coefficients using the fraction of bacteria recovered from laboratory columns. Environ Sci Technol 32:1329–1332
Bolton EW, Lasaga AC, Rye DM (1996) A model for the kinetic control of quartz dissolution and precipitation in porous media flow with spatially variable permeability: formulation and examples of thermal convection. J Geophys Res 101:22157–22187
Bolton EW, Lasaga AC, Rye DM (1997) Dissolution and precipitation via forced-flux injection in the porous medium with spatially variable permeability: kinetic control in two dimensions. J Geophys Res 102:12159–12172
Camesano T, Logan B (1998) Influence of fluid velocity and cell concentration on the transport of motile and non-motile bacteria in porous media. Environ Sci Technol 32:1699–1708
Cheng JT, Pyrak-Nolte LJ, Nolte DD, Giordano NJ (2004) Linking pressure and saturation through interfacial areas in porous media. Geophys Res Lett 31:L08502
Cortis A, Harter T, Hou L, Atwill ER, Packman AI, Green PG (2006) Transport of *Cryptosporidium parvum* in porous media: long-term elution experiments and continuous time random walk filtration modeling. Water Resour Res 42:W12S13
Daccord G (1987) Chemical dissolution of a porous medium by a reactive fluid. Phys Rev Lett 58:479–482
Daccord G, Lenormand R (1987) Fractal patterns from chemical dissolution. Nature 325:41–43
Daccord G, Lietard O, Lenormand R (1993) Chemical dissolution of a porous medium by a reactive fluid, 2, Convection vs. reaction behavior diagram. Chem Eng Sci 48:179–186
Darmody RG, Thorn CE, Harder RL, Schlyter JPL, Dixon JC (2000) Weathering implications of water chemistry in an arctic-alpine environment, North Sweden. Geomorphol 34:89–100
Dijk P, Berkowitz B (1998) Precipitation and dissolution of reactive solutes in fractures. Water Resour Res 34:457–470
Dijk P, Berkowitz B (2000) Buoyancy-driven dissolution enhancement in rock fractures. Geol 28:1051–1054
Eliott AH, Trowsdale SA (2007) A review of models for low impact urban stormwater drainage. Environ Mod Softw 22:394–405
Emmanuel S, Berkowitz B (2005) Mixing-induced precipitation and porosity evolution in porous media. Adv Water Resour 28:337–344
Ewing RP, Berkowitz B (1998) A generalized growth model for simulating initial migration of dense non-aqueous liquids. Water Resour Res 34:611–622
Fogler HS, Rege SD (1986) Porous dissolution reactors. Chem Eng Commun 42:291–313
Furuberg L, Feder J, Aharony A, Jøssang T (1988) Dynamics of invasion percolation. Phys Rev Lett 61:2117–2120
Hairsine PB, Rose CW (1991) Rainfall detachment and deposition: modeling the physical processes. Proc Soil Sci Soc Am 55:320–324
Hilgers C, Urai JL (2002) Experimental study of syntaxial vein growth during lateral fluid flow in transmitted light: first results. J Struct Geol 24:1029–1043
Hoefner ML, Fogler HS (1988) Pore evolution and channel formation during flow and reaction in porous media. AIChE J 34:45–54
Hornung G, Berkowitz B, Barkai N (2005) Morphogen gradient formation in a complex environment: an anomalous diffusion model. Phys Rev E 72:041916
Hubbard RK, Erickson AE, Ellis BG, Wolcot AR (1982) Movement of diffuse source pollutants in small agricultural watersheds of the Great Lakes Basin. J Environ Qual 11:117–123
Israelachvili JN (1991) Intermolecular and surface forces. Elsevier, New York
Jain V, Bryant S, Sharma M (2003) Influence of wettability and saturation on liquid–liquid interfacial area in porous media. Environ Sci Technol 37:584–591

Johns ML, Gladden LF (1999) Magnetic resonance imaging study of the dissolution kinetics of octanol in porous media. J Colloid Interface Sci 210:261–270
Jové Colon CF, Oelkers EH, Schott J (2004) Experimental investigation of the effect of dissolution on sandstone permeability, porosity, and reactive surface area. Geochim Cosmochim Acta 68:805–817
Jury WA, Fluhler H (1992) Transport of chemicals through soil: mechanisms, models and field applications. Adv Agron 47:142–202
Kieffer B, Jové CF, Oelkers EK, Schott J (1999) An experimental study of the reactive surface area of the Fontainebleau sandstone as a function of porosity, permeability, and fluid flow rate. Geochim Cosmochim Acta 63:3525–3534
Lasaga A (1984) Chemical kinetics of water-rock interactions. J Geophys Res 89:4009–4025
Lee YJ, Morse JW (1999) Calcite precipitation in synthetic veins: implications for the time and fluid volume necessary for vein filling. Chem Geol 156:151–170
Lenormand R, Zarcone C (1985) Invasion percolation in an etched network: measurement of fractal dimension. Phys Rev Lett 54:2226–2229
Lenormand R, Touboul E, Zarcone C (1988) Numerical models and experiments on immiscible displacement in porous media. J Fluid Mech 189:165–187
Lichtner PC (1988) The quasistationary state approximation to coupled mass transport and fluidrock interaction in porous media. Geochim Cosmochim Acta 52:143–165
Logan BE, Jewett DG, Arnold RG, Bouwer EJ, Omelia CR (1995) Clarification of clean-bed filtration models. J Environ Eng ASCE 121:869–873
Margolin G, Dentz M, Berkowitz B (2003) Continuous time random walk and multirate mass transfer modeling of sorption. Chem Phys 295:71–80
Martin MJ, Logan BE, Johnson WP, Jewett DG, Arnold RG (1996) Scaling bacterial filtration rates in different sized porous media. J Environ Eng 122:407–415
McDowell LL, Willis GH, Murphree CE (1984) Plant nutrient yields in runoff from a Mississippi delta watershed. Trans ASAE 27:1059–1066
McDowell-Boyer L, Hunt JR, Sitar N (1986) Particle transport through porous media. Water Resour Res 22:1901–1921
Menzel RG, Rhoade ED, Onless AE, Smith SJ (1978) Variability of annual nutrient and sediment discharge in runoff from Okalahoma cropland and rangeland. J Environ Qual 7:401–406
Michaelides K, Wilson MD (2007) Uncertainty in predicted runoff due to patterns of spatially variable infiltration. Water Resour Res 43:W02415
Miller CT, Poirier-McNeill MM, Mayer AS (1990) Dissolution of trapped nonaqueous phase liquids: mass transfer characteristics. Water Resour Res 26:2783–2796
Morse JW, Arvidson RS (2002) The dissolution kinetics of major sedimentary carbonate minerals. Earth Sci Rev 58:51–84
Novak CF (1993) Modelling mineral dissolution and precipitation in dual-porosity fracture-matrix system. J Contam Hydrol 13:91–115
Novak CF, Lake LW (1989) Diffusion and solid dissolution/precipitation in permeable media. AIChE J 35:1057–1072
Ovdat H, Berkowitz B (2006) Pore-scale study of drainage displacement under combined capillary and gravity effects in index-matched porous media. Water Resour Res 42:W06411
Palmer AN (1996) Rates of limestone dissolution and calcite precipitation in cave streams of east-central New York state, northern section. Geol Soc Am 28:89
Powers SE, Abriola LM, Weber WJ Jr (1992) An experimental investigation of nonaqueous phase liquid dissolution in saturated subsurface systems—steady state mass transfer rates. Water Resour Res 28:2691–2705
Proffitt APB, Rose CW, Hairsine PB (1991) Rainfall detachment and deposition. Experiments with low slopes and significant water depth. Soil Sci Soc Am J 55:325–332
Rajagopalan R, Tien C (1976) Trajectory analysis of deep bed filtration with the sphere-in-cell porous media model. AIChE J 3:523–533
Redman JA, Grant SB, Olson TM, Estes MK (2001) Pathogen filtration, heterogeneity, and the potable reuse of wastewater. Environ Sci Technol 35:1798–1805

Redman JA, Walker SL, Elimelech M (2004) Bacterial adhesion and transport in porous media: role of the secondary energy minimum. Environ Sci Technol 38:1777–1785

Reeves CP, Celia MA (1996) A functional relationship between capillary pressure, saturation, and interfacial area as revealed by a pore-scale network model. Water Resour Res 32:2345–2358

Rose CW (1993) The transport of adsorbed chemicals in eroded sediments. In: Russo D, Dagan G (eds) Water flow and solute transport in soils. Springer, Heidelberg, pp 180–199

Rubin S, Dror I, Berkowitz B (2012) Experimental and modeling analysis of coupled non-Fickian transport and sorption in natural soils. J Contam Hydrol 132:28–36

Ryan JN, Elimelech M (1996) Colloid mobilization and transport in groundwater. Colloids Surf A 107:1–56

Saiers JE, Hornberger GM (1996) The role of colloidal kaolinite in the transport of cesium through laboratory sand columns. Water Resour Res 32:33–41

Saripalli PK, Kim H, Suresh P, Rao C, Annable DM (1997) Measurements of specific fluid–fluid interfacial areas of immiscible fluids in porous media. Environ Sci Technol 31:932–936

Schaefer C, DiCarlo DA, Blunt MJ (2000) Determination of water–oil interfacial area during three-phase gravity drainage in porous media. J Colloid Interface Sci 221:308–312

Schwille F (1988) Dense chlorinated solvents in porous and fractured media. Lewis Publishers CRC Press, Boca Raton

Singurindy O, Berkowitz B (2003) Evolution of hydraulic conductivity by precipitation and dissolution in carbonate rock. Water Resour Res 39:1016

Starr RC, Gillham RW, Sudicky EA (1985) Experimental investigation of solute transport in stratified porous media: the reactive case. Water Resour Res 21:1043–1050

Toride N, Leij F, van Genuchten M (1995), The CXTFIT code for estimating transport parameters from laboratory or field tracer experiments, version 2.0. Res. Rep. 137, U.S. Salinity Lab, Riverside

Tufenkji N, Elimelech M (2004) Correlation equation for predicting single-collector efficiency in physicochemical filtration in saturated porous media. Environ Sci Technol 38:529–536

Wallach R, Grogorin G, Rivlin (Byk) J (1997) The errors in surface runoff prediction by neglecting the relationship between infiltration rate and overland flow depth. J Hydrol 200:243–259

Walton RS, Volker RE, Bristow KL, Smettem KRJ (2000) Experimental examination of solute transport by surface runoff from low-angle slopes. J Hydrol 233:19–36

Wiesner MR, Characklis G, Brejchova D (1995) Colloidal contaminants in urban runoff. In: Proceedings of the 21st annual RREL research symposium, Cincinnati, OH, April, United State Environmental Protection Agency, EPA/600/R-95/012

Wilkinson D (1984) Percolation model of immiscible displacement in the presence of buoyancy forces. Phys Rev A 30:520–531

Wilkinson D (1986) Percolation effects in immiscible displacement. Phys Rev A 34:1380–1391

Wilkinson D, Willemsen JF (1983) Invasion percolation: a new form of percolation theory. J Phys A 34:1380–1391

Yao K-M, Habibian MT, O'Melia CR (1971) Water and waste water filtration: concepts and applications. Environ Sci Technol 5:1105–1112